

Measurement of pelvic osteolytic lesions in follow-up studies after total hip arthroplasty

Benjamin Castaneda^{a*}, Jose Gerardo Tamez-Pena^b, Saara Totterman^b, Regis O'Keefe^c, R. John Looney^d

^aDepartment of Electrical & Computer Eng., University of Rochester, Rochester, NY USA 14627

^bVirtualScopics, LLC, 350 Linden Oaks, Rochester, NY USA 14625

^cDepartment of Orthopedics and ^dDepartment of Medicine, University of Rochester Medical Center, Rochester, NY USA 14642

ABSTRACT

Previous studies have demonstrated the plausibility of using volumetric computerized tomography to provide an accurate representation and measurement of volume for pelvic osteolytic lesions following total hip joint replacement. These studies have been performed manually (or computed-assisted) by expert radiologists with the disadvantage of poor reproducibility of the experiment. The purpose of this work is to minimize the effect of user interaction in these experiments by introducing Laplacian level set methods in the volume segmentation process and using temporal articulated registration in order to follow the evolution of a lesion over time. Laplacian level set methods reduce the inter and intra-observer variability by attaching the segmented contour to edges defined in the image while keeping smoothness. The registration process allows the information of the lesion from the first visit to be used in the segmentation process of the current visit. This work compares the automated results on 7 volunteers versus the volume measured manually. Results have shown that the proposed technique is able to track osteolytic lesions and detect changes in volume over time. Intra-reader and inter-observer variabilities were reduced.

Keywords: Pelvic osteolytic lesion, analysis and quantification, volume measurement, segmentation, 3D registration, Laplacian level set methods.

1. INTRODUCTION

Total hip arthroplasty (THA) is an orthopedic surgery which highly improves the quality of life and relieves pain for patients with end-stage hip disease. The number of THAs performed each year has been estimated over 1.5 million. One of the major long-term complications of THA is periprosthetic osteolysis, which frequently progresses to failure of fixation. This process, known as aseptic loosening, is the primary reason for revision of THA. It has been postulated that wear-debris-induced osteolysis is the major cause of prosthetic implant failure^{1,2,3,4}. It is hypothesized that wear debris generated from the prosthesis is phagocytosed by macrophages, which then initiate an inflammatory response. This leads to the recruitment of activated osteoclasts, which cause osteolysis at the bone-implant interface. Studies with animal models have been developed, both to understand this process, and to evaluate potential interventions^{5,6,7,8}. In these experimental models, quantitative analysis of histologic parameters provides direct measurement of osteolysis. These techniques, however, are not applicable to human investigations. Although radiologic analysis is a direct measure, the current methodology is insensitive and subject to operator error. Plain radiographic analysis is a two-dimensional measurement of a process that occurs in three dimensions; the complex three-dimensional (3D) structure of the pelvic bone prevents its use in the periacetabular area. Previous studies^{9,10} have demonstrated the plausibility of using volumetric computerized tomography to provide an accurate representation and measurement of volume for pelvic osteolytic lesions following total hip joint replacement. These studies have been performed manually (or computed-assisted) by expert radiologists with the disadvantage of poor reproducibility of the experiment. The purpose of this work is to minimize the effect of user interaction in these experiments by introducing level set methods in the volume segmentation process and using temporal registration in order to follow the evolution of a lesion over time.

* castaned@ece.rochester.edu; phone 585-748-3744

2. MATERIALS AND METHODS

A study of nine subjects with three visits per subject after total hip joint replacement was performed. The time difference between consecutive visits was 6 months. In each visit, a CT volume was acquired and processed to reduce the streak artifacts caused by the metal implants. Each one of the CT processed volumes was reviewed by an expert radiologist who manually segmented the pelvic osteolytic lesions. The manual segmentation of the first visit was refined using Laplacian level set segmentation which delivered the final volume for the lesion in the first visit. In order to measure automatically the same lesion in the follow-up studies, an articulated registration process was performed between the first and second visit, and between the first and third visits. The result of the registration was used to transform the volume of the lesion in the first visit to the second one. Then, a Laplacian level set segmentation was performed to obtain the measure of the lesion in the second visit. The same process was repeated for the third visit to obtain the final measure of the lesion. An overview of the procedure is given in Figure 1.

2.1. Human subjects

Subjects were enrolled as part of a randomized, placebo-controlled, double-blind study of Enbrel[®] (Etanercept, Immunex Corp., Seattle, Washington, USA) for prosthetic hip loosening. Patients with X-ray evidence of acetabular loosening on plain X-ray films were recruited from the clinical practice of the Department of Orthopedics at the University of Rochester (Rochester, NY, USA). Subjects that had an uncemented acetabular component, were ambulatory, and were at least five years post implant were eligible for this study. Exclusion criteria included inflammatory arthritis, history of prosthetic joint infection, current active infection, severe medical illness, chronic use of systemic glucocorticoids, use of calcitonin, and metabolic bone disease (except osteoporosis). Informed consent was obtained from all subjects. The Human Subjects Review Board of the University of Rochester approved this study. Plain X-rays and CT studies were performed on all patients.

2.2. Algorithm description

The first step in the algorithm is to process the CT volumes in order to suppress streak artifacts caused by the hip prosthesis. The artifacts were corrected using the a proprietary software for metal artifact reduction³ (Virtualscopics LLC, Rochester, New York). Then, an expert radiologist manually segmented the lesions in the CT images from the first visits. The CT volumes for the three visits plus the radiologist manual segmentation of the first visit are the input for the algorithm. From this point, an automatic process produces the final segmentation for the three visits following the procedure described in Figure 1. In the next subsections, the descriptions of the temporal registration algorithm and the Laplacian level set segmentation are presented.

2.2.1. Temporal registration

The goal of the temporal registration is to create dense motion fields between the registered images. In our case, between the first and second visits, and between the first and third visits. The dense motion fields describe the three-dimensional displacement that every voxel in the base image undergoes to be represented in the coordinate system of the registered image. Using these fields, the segmentation for the first visit is temporally registered to the second and third visits.

To create the dense motions fields, the algorithm presented by Tamez-Pena *et al.*¹¹ is followed. The first CT volume is processed with a 3D segmentation algorithm based in a hybrid linkage region growing scheme, where every voxel in the volume is regarded as a node in a graph. Neighboring voxels whose properties are similar enough are joined by an arc forming a region. The regions in the segmented image are then manually relabeled into *pelvic bone*, *prosthetic cup* and *other*. Based on this segmentation a coarse FEM mesh is created. The stiffness of the elements is selected according to the region to which they belong. Following an energy minimization process the displacement for every point in the mesh is obtained. Finally, this displacement is interpolated to create the dense motion field.

2.2.2. Laplacian level set segmentation

Level set methods are numerical techniques for tracking the evolution of interfaces (contours or surfaces). The interface is embedded as the zero level set of a higher dimensional function called the level-set function, $\Psi(X, t)$. The level-set function is then evolved and its behavior is defined by the following differential equation in a general case:

$$\frac{d}{dt} \Psi = -\alpha A(x) \cdot \nabla \Psi - \beta P(x) |\nabla \Psi| + \gamma C(x) \kappa |\nabla \Psi| = 0 \quad (1)$$

Where A is an advection term, P is a propagation term, and C is a spatial modifier term for the mean curvature κ . The scalar constants α , β , and γ are weights that determine the relative influence of each of the terms on the evolution of the interface.

The evolving interface is obtained at any given time iteration by extracting the zero level set from the higher dimensional function. The main advantages of these techniques are that arbitrarily complex shapes can be modeled and topological changes are handled implicitly.

In the case of Laplacian level set methods the propagation term is calculated as the Laplacian of the image values. As a consequence, the evolving level set surface will be attracted to local zero-crossings in the Laplacian image. This is a suitable property to refine existing segmentations which is the case in the present work. The curvature term controls the smoothness of the contour. For our experiments γ was set to 1, β was set to 0.2 and $\alpha=0$ since the advection term is not required. The curvature term is given 5 times more importance than the propagation term in order to avoid leakage in the contour at places where the lesion edge is not well defined. Figure 2 shows how the Laplacian level set segmentation works. The initial (manual) segmentation is evolved and attracted to the edges of the image defined by the Laplacian of the CT Image. For more information about level set methods and their applications, the reader is directed to an overview of the field by Sethian¹².

2.3. Experiments

The proposed algorithm for volumetric measurements needs to be initialized with a manual segmentation. This segmentation is refined by using Laplacian level set methods with the goal of reducing the inter and intra-observer variability. To test this hypothesis, 2 expert radiologists were asked to segment lesions for 3 patients from the database. Each patient was presented to each radiologist 5 times. The Laplacian level set segmentation was applied to each of the 15 cases and the inter-observer and intra-observer variability was computed for manual segmentation and for Laplacian level set segmentation. The root-mean-square error is used to compare the methods and a paired t-test is performed to evaluate for statistical significance.

The complete volumetric measurement procedure was applied to the CT images of 9 patients. An expert radiologist manually segmented the lesion on CT volumes for the three visits. The manual segmentations are compared to the ones created by the algorithm. Since the time between consecutive visits is six months, the ability to detect changes in this amount of time is tested and plotted in a Bland-Altman graph. The coefficient of variability is computed.

The analysis of all the experiments was performed over the cubic root of the volumes found. Therefore the results are reported in units of length (mm).

3. RESULTS

3.1. Intra-observer and inter-observer

The objective evaluation of the algorithm performance was done by a direct comparison of the results to the inter-observer performance of the current system. The inter-performance analysis was done using 14 data sets that were

randomly analyzed by two independent trained users. The results of this blinded analysis yield that the diameter of the lesion can be determined with a precision of 2.3mm. Figure 4 shows the Bland-Altman plot of the inter-observer result. Three subjects of the set were used for the direct intra and inter performance of the algorithm. Those subjects were analyzed by the algorithm and the two observers (3 patients, 2 observers). From the six cases, the use of Laplacian level set segmentation reduced the variability in four. One case remained unchanged and in one case the variability was increased. For the inter-observer analysis, the variability was indeed reduced for the three patients. Figure 3 shows the root-mean-square error for both analyses. In the intra-observer case, the Laplacian level set segmentation reduces the rms error from 2.31mm to 2.17mm. The differences in the observer interpretation were estimated by taking the average value of the measurements and then computing the inter-observer variability. The inter-observer rms error was reduced from 1.67mm to 1.52mm. Although these results are promising, they are not statistically significant and more studies are needed.

3.2. Follow-up Studies

The algorithm was successfully applied to the CT images of 7 patients. The motion fields created for the remaining two patients failed to register the segmentation of the first visit into the volumes of the next two visits. The average length for the lesions in the three visits was 20.66mm. The average difference of lesion length between consecutive visits was 0.56mm. The standard deviation of the differences was 0.62mm. The coefficient of variability was 2.1%. Figure 5 shows the Bland-Altman graph which indicates the change (growth) of the lesion in function of its size.

The same analysis was performed over the manually segmented lesions for the 9 patients. The average length was 28.3mm. The average difference of lesion length between visits was 0.51mm. The standard deviation of the difference was 2.11mm. The coefficient of variability was 5.26%. Figure 6 shows the Bland-Altman graph for the manual segmentation. The graph indicates the change (growth) of the lesion in function of its size.

4. DISCUSSION

This work presents a new approach for semi-automatic measurement of pelvic osteolytic lesions in follow-up studies after total hip arthroplasty using computerized volumetric tomography. The approach takes advantage of the data collected in the patient's first visit to measure automatically the volume of the lesion in the follow-up visits. Studies of the Laplacian level set segmentation indicate that the intra-observer and inter-observer reproducibility is increased. These results, although promising, are not statistically significant.

The Bland-Altman plot for the proposed algorithm (Figure 5) shows the change in the lesion vs. the size of the lesion. Although more data is required to validate the algorithm, the preliminary analysis shows that smaller lesions have a relative bigger growth over a six month period. This is consistent with current lesion evolution hypothesis. Growth in smaller regions is not restricted while bigger regions are confined by the cortical bone. The graph shows that the lesions are growing over time, which is the expected behavior.

The Bland-Altman plot for the manually segmented lesions over time (Figure 6) presents the same tendency as the plot for the proposed algorithm (Figure 5): Smaller lesions have a relative bigger growth than larger lesions. However, it also shows several measurements in which the volume of the lesion has decreased over a 6 months period which is contradictory to current lesion evolution hypothesis.

The longitudinal analysis done using the computerized approach indicates that it improved the manual performance by three times. The experiments presented in this study showed that the variability of the manual methods are poor with a length reproducibility in the order of 1.5mm while the combination of Laplacian level set segmentation with temporal registration has an error of 0.44mm in the lesion length. Therefore now it is possible to detect length changes greater than 0.88 mm by CT.

5. CONCLUSION

This work presented the use of articulated registration and Laplacian level set segmentation to increase the reproducibility of pelvic osteolytic lesion measurements on longitudinal studies. The results showed the reduction of intra-observer and inter-observer variability. Moreover, the results demonstrated the capacity of the algorithm to follow the changes in volume of the lesions. The performance of the longitudinal analysis was improved from an error of 1.5 mm to a longitudinal variation of just 0.44mm. Future work will focus on fully understanding the performance of the system using a bigger sample size and in the automatic detection of lesions to further minimize human interaction, and the overall variability.

ACKNOWLEDGEMENTS

Support for this project has been provided by a research grant from the NIH, NIAMS AR48149. This work was supported in part by a General Clinical Research Center Grant, 5MO1-R00044, from the National Center for Research Resources, NIH. The authors are also thankful to Prof. Kevin J. Parker for the fruitful discussions of the topic with him.

REFERENCES

1. Horowitz SM, Doty SB, Lane JM, Burstein AH. "Studies of the mechanism by which the mechanical failure of polymethyl-methacrylate leads to bone resorption". *J Bone Joint Surg Am.*; **75**:802–813, 1993.
2. al-Saffar N, Revell PA. "Interleukin-1 production by activated macrophages surrounding loosened orthopedic implants: a potential role in osteolysis". *Br J Rheumatol.*; **33**:309–316, 1994.
3. Kadoya Y, Revell PA, al-Saffar N, Kobayashi A, Scott G, Freeman MA. "Bone formation and bone resorption in failed total joint arthroplasties: histomorphometric analysis with histochemical and immunohistochemical technique". *J Orthop Res.*; **14**:473–482, 1996.
4. Glant TT, Jacobs JJ. "Response of three murine macrophage populations to particulate debris: bone resorption in organ cultures". *J Orthop Res.*; **12**:720–731, 1994.
5. Howie DW, Vernon-Roberts B, Oakeshott R, Manthey B. "A rat model of resorption of bone at the cement-bone interface in the presence of polyethylene wear particles". *J Bone Joint Surg Am.*; **70**:257–263, 1988.
6. Schwarz EM, Benz EB, Lu AL, Goater JJ, Mollano AV, Rosier RN, Puzas JE, O'Keefe RJ. "A quantitative small animal surrogate to evaluate drug efficacy in preventing wear debris-induced osteolysis". *J Orthop Res.*; **18**:849–855, 2000.
7. Shanbhag AS, Hasselman CT, Rubash HE. "Inhibition of wear debris mediated osteolysis in a canine total hip arthroplasty model". *Clin Orthop.*; **344**:33–43, 1997.
8. Pap G, Machner A, Rinnert T, Horler D, Gay RE, Schwarzberg H, Neumann W, Michel BA, Gay S, Pap T. "Development and characteristics of a synovial-like interface membrane around cemented tibial hemiarthroplasties in a novel rat model of aseptic prosthesis loosening". *Arthritis Rheum.*; **44**:956–963, 2001.
9. Claus AM, Totterman SM, Sychterz C, Tamez-Peña JG, Looney RJ, Engh CA, "The Accuracy of Computed Tomography in Determining Location and Size of Pelvic Osteolysis Following Total Hip Arthroplasty: A Cadaver Study". *Clin. Orthop.*; **422**: 167-174, 2004.
10. Looney RJ, Boyd A, Totterman S, Seo G, Tamez-Pena JG, Campbell D, Novotny L, Olcott C, Martell J, Hayes FA, O'Keefe RJ, Schwarz EM. "Volumetric computerized tomography as a measurement of periprosthetic acetabular osteolysis and its correlation with wear". *Arthritis Research*; **4**:59-63, 2002.
11. Tamez-Pena JG, Parker KJ, Totterman S. "The integration of Automatic Segmentation and Motion Tracking for 4D Reconstruction and Visualization of Muculoskeletal Structures". *Proceedings of the IEEE workshop on Biomedical Image Analysis*, pp. 154-163, Santa Barbara, CA., 1998
12. J.A. Sethian. *Level Set Methods and Fast Marching Methods*. Cambridge University Press, New York, 1999.

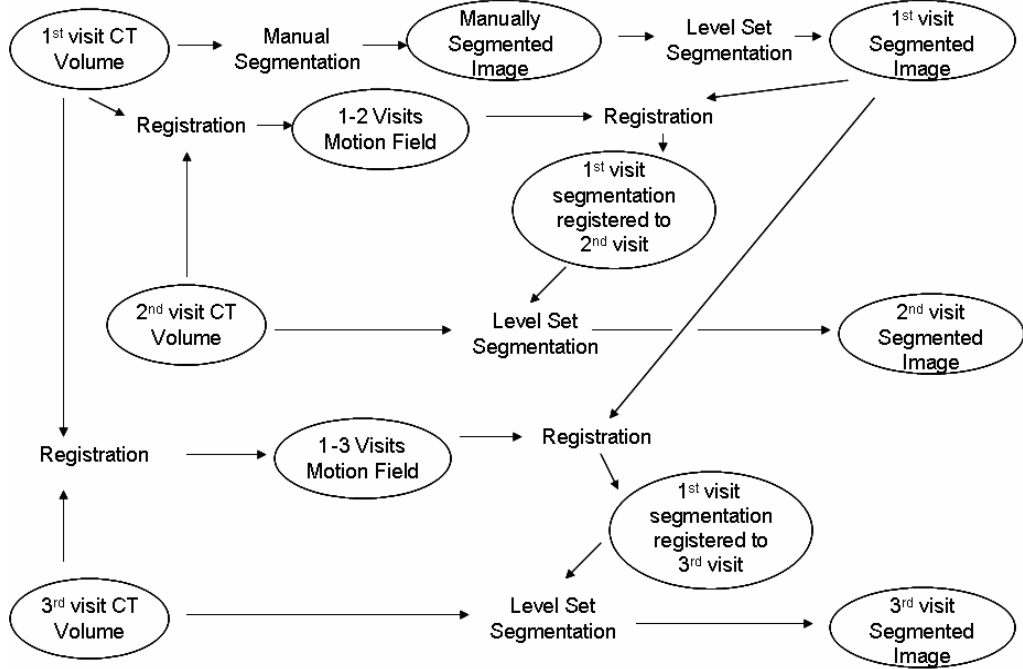


Figure 1: Algorithm overview

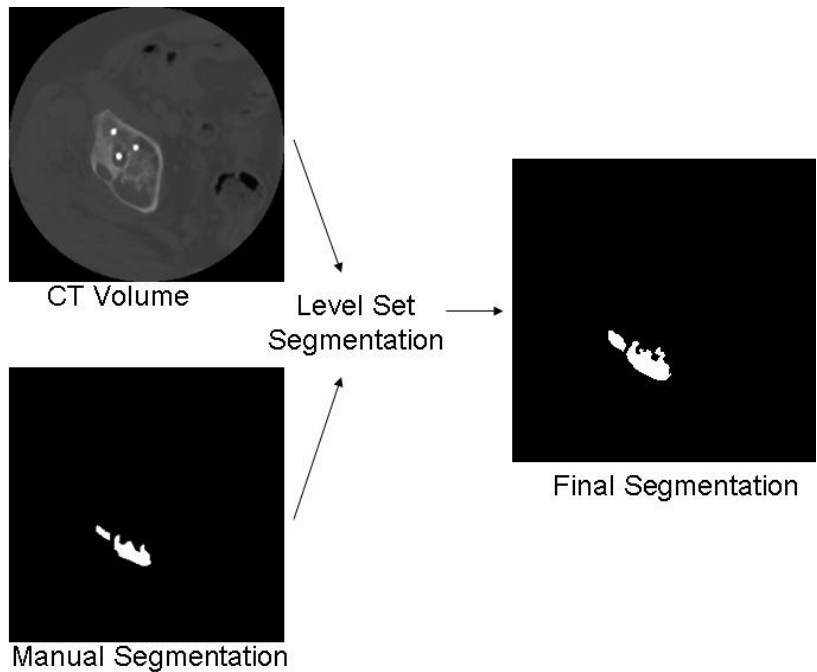


Figure 2: Level Set Segmentation

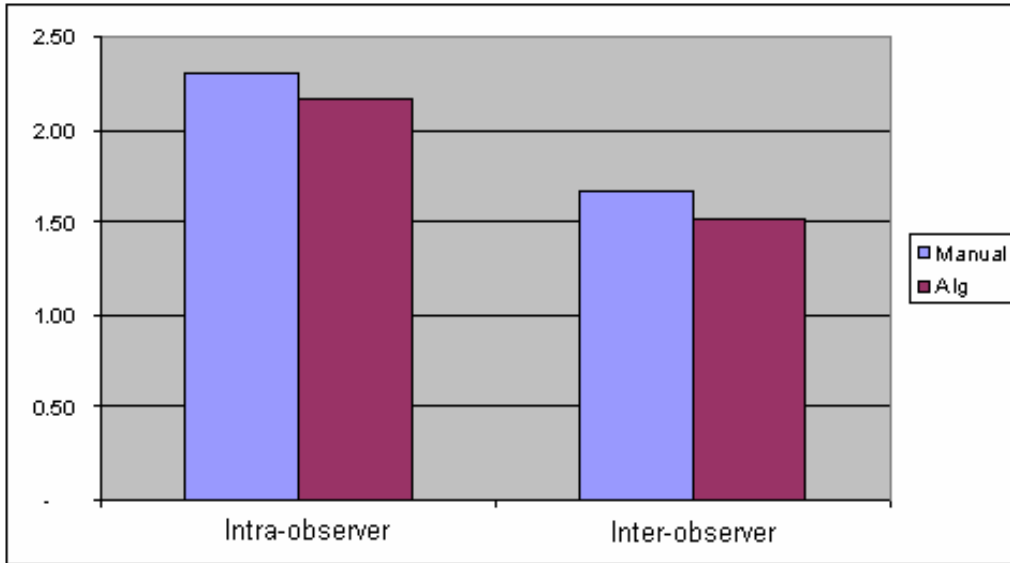


Figure 3: RMS error for intra-observer and inter-observer experiments expressed in mm

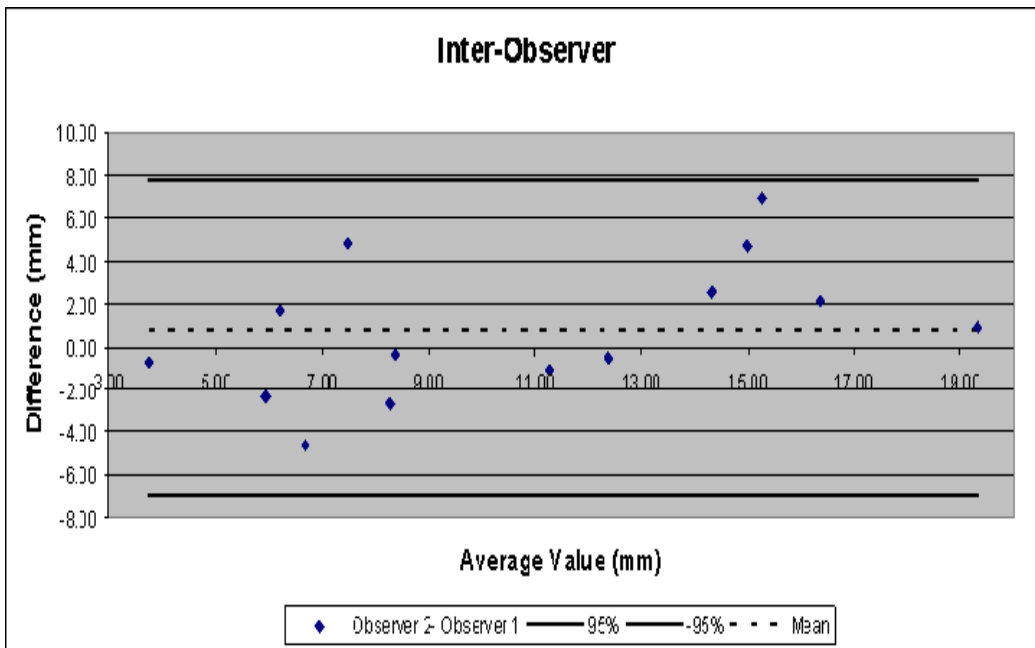


Figure 4: Bland-Altman plot for manually segmented lesions in the inter-observer cases

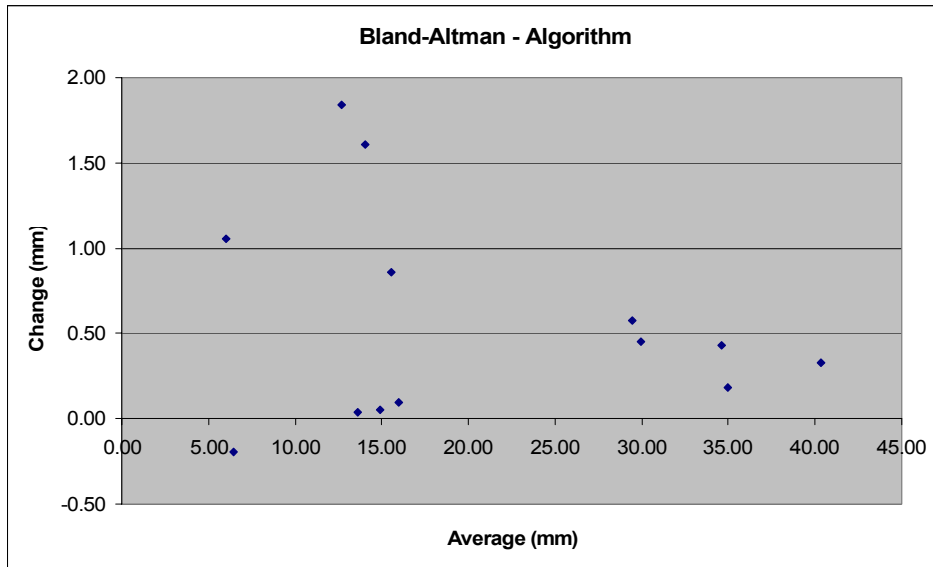


Figure 5: Bland-Altman plot for lesions segmented by the algorithm in the longitudinal study

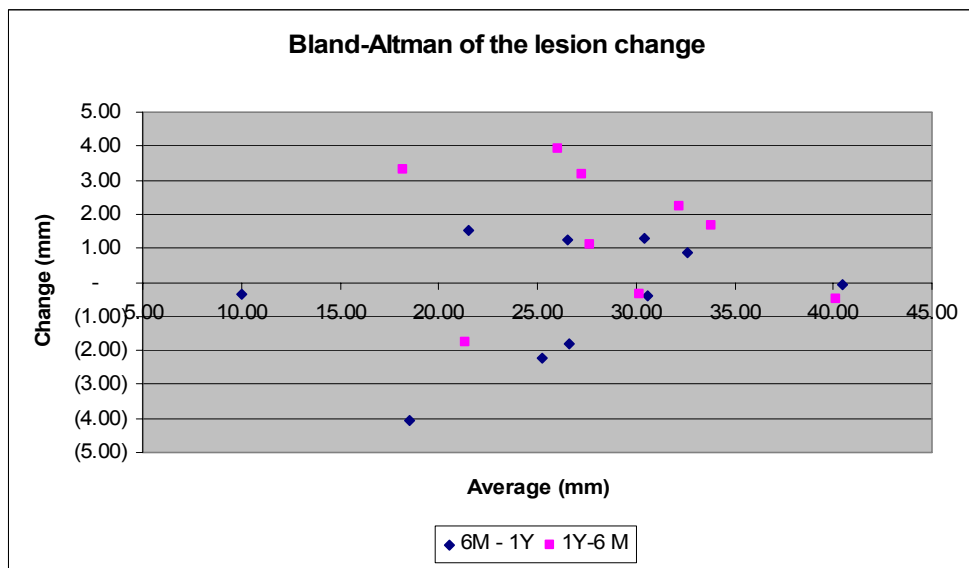


Figure 6: Bland-Altman plot for manually segmented lesions in the longitudinal study